Journal of Power Sources 247 (2014) 920–931

Contents lists available at ScienceDirect

Journal of Power Sources

journal homepage: www.elsevier.com/locate/jpowsour

Review

Spark plasma sintered/synthesized dense and nanostructured materials for solid-state Li-ion batteries: Overview and perspective

Ravi Kali, Amartya Mukhopadhyay*

High Temperature and Energy Materials Laboratory, Department of Metallurgical Engineering and Materials Science, IIT Bombay, Powai, Mumbai 400076, India

HIGHLIGHTS

- First review demonstrating the fabrication of solid-state Li-ion batteries via SPS.
- SPS allows phase stability and enhanced ionic conductivity for solid electrolytes.
- 'Superior' grain boundaries lead to such enhanced ionic conductivities.
- SPS allows synthesis of nanosized cathode particles with enhanced rate capability.
- Further possible advancements in Li-ion battery technology using SPS highlighted.

ARTICLE INFO

Article history:
Received 30 July 2013
Received in revised form
2 September 2013
Accepted 3 September 2013

Keywords:
Spark plasma sintering
Solid electrolyte
Ionic conductivity
All-solid-state Li-ion battery

ABSTRACT

Spark Plasma Sintering (SPS) offers advantages that include faster densification, activated materials synthesis, formation of atomically clean grain boundaries, good grain-to-grain bonding, and minimization of particle coarsening that allows the retention of nanosized grains/particles during synthesis or sintering. The present review summarizes for the first time the possibilities of using these advantages for applications in electrochemical energy storage, or more precisely, for developing high performance all-solid-state Li-ion batteries that are better suited for more heavy duty applications, such as in automobiles. This survey demonstrates the improvements that can be achieved for the ionic conductivities of the ceramic solid electrolytes on sintering via SPS and for the overall transport properties of the cathode materials on synthesizing via SPS. These would not only render the solid electrolytes better suited for enhanced practical applications, but also result in overall improved rate capabilities for the batteries. Furthermore, possibilities of fabricating entire solid-state Li-ion batteries, possessing improved mechanical integrity and power density, via one-step SPS of stacked laminates of anode–solid electrolyte–cathode materials have been brought into light. The improvements achieved, mainly due to the formation of 'perfect' interfaces and due to nanostructuring, are correlated to the intrinsic mechanisms of the spark plasma sintering process.

1. Introduction

Spark plasma sintering (SPS) is an advanced sintering technique, which utilizes simultaneous applications of uniaxial pressure and pulsed direct electrical current (pulsed DC) to densify powder compacts [1–5]. The heating rates (up to 600 °C min^{-1}) achieved in SPS are more than an order of magnitude greater than that achieved with the more conventional sintering techniques. Furthermore, near theoretical sinter-densities can be achieved even with significantly lower holding times (in most cases 0–10 min) for conducting, as well as non-conducting powder compacts, and even for the inherently difficult-to-sinter materials, such as transition metal borides [1,5–8]. Reports also suggest that such densification can be achieved at temperatures that are lower by 200–300 °C compared to the more conventional sintering techniques, which however is controversial [1,6]. Nevertheless, it has been demonstrated time and again [1–8] that SPS can successfully minimize particle/grain coarsening during densification, which in turn routinely allows the successful fabrication of dense 3D nanomaterials in various research laboratories. In addition to sintering, SPS has also been used to achieve faster reaction kinetics, and

* Corresponding author. Tel.: +91 22 25767612; fax: +91 22 25766975.
E-mail addresses: amartya_mukhopadhyay@iitb.ac.in, amartya.28nov@gmail.com (A. Mukhopadhyay).

0378-7753/$ – see front matter © 2013 Elsevier B.V. All rights reserved.
http://dx.doi.org/10.1016/j.jpowsour.2013.09.010

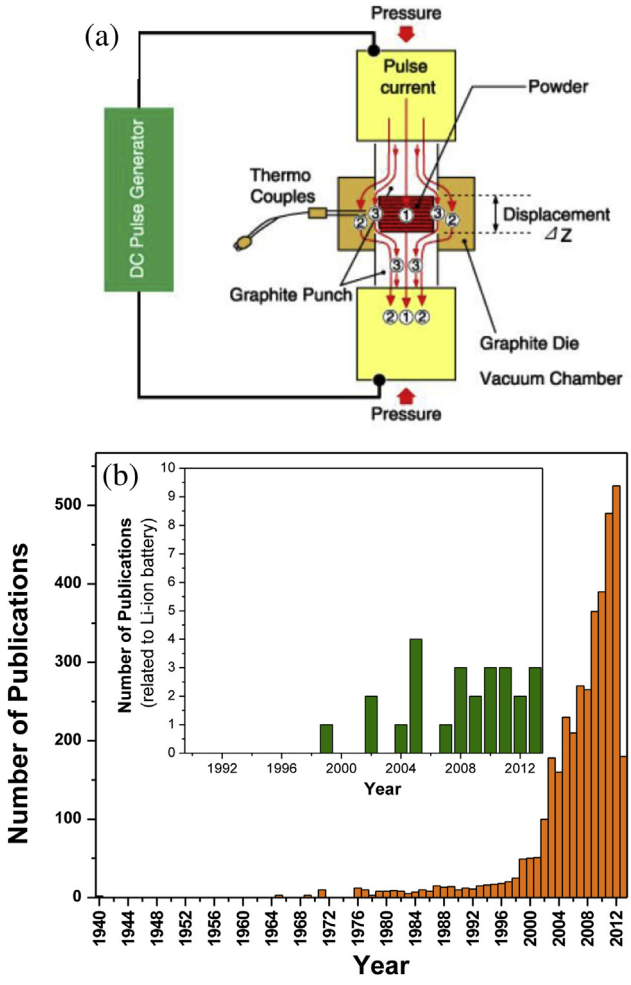

Fig. 1. (a) Schematic representation of the spark plasma sintering (SPS) equipment, showing the various important parts [1], and (b) plot showing the approximate number of publications based on SPS per year, from 1940 till early 2013 [5,12]. The inset of (b) presents the numbers of corresponding publications related to Li-ion batteries.

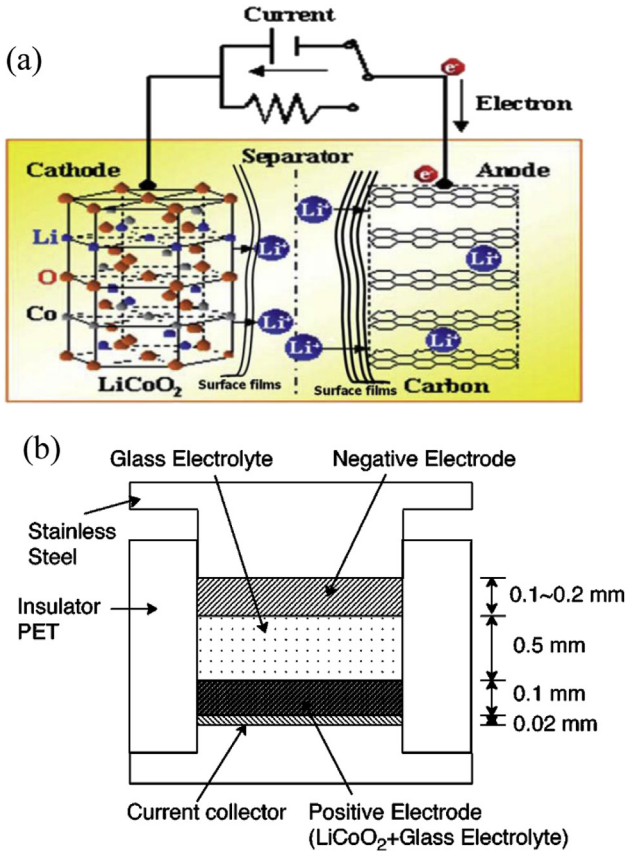

Fig. 2. Schematic representations of the typical constructions of (a) more conventional Li-ion cell (containing liquid electrolyte), showing the basic redox processes [33] and (b) all-solid-state Li-ion battery (containing ceramic solid electrolyte) [34].

hence activated synthesis of different materials from precursors [3,6,9]. Fig. 1a presents a schematic representation of the spark plasma sintering equipment. The basic principles and mechanistic aspects of SPS have been extensively described in earlier reviews [1–5].

Use of DC for sintering of mainly metallic (conducting) powders, via a process called resistance sintering (RS), has been known since 1906 [5,10]. However, the use of pulsed DC to generate spark and possible plasma between the powder particles, a mechanism on which the modern day SPS is based on, came to the fore in the early 1960s in Japan and was used to improve the sinterability, also of nonmetallic (ceramic) powders [5,11,12]. Following the realization of the fact that with improved processibility and microstructure control, ceramics, in particular nanoceramics, ceramic nanocomposites [1,4] and ultra-high temperature ceramics [5–8], can be used for advanced structural applications, the 1990s saw initiation of extensive and continuing research on the sintering of ceramics via SPS. Before the turn of the century, SPS was used for sintering various types of materials, but primarily for structural applications. Over the last decade, it has been realized that the advantages offered by SPS result in improved materials' performance not only for structural applications [1–8], but also for functional applications [4,5], including electronic and biological applications. Accordingly, the number of publications related to SPS, which was increasing considerably from the early 1990s, saw a near exponential increase over the last decade (see Fig. 1b). Very recently, it has been demonstrated that SPS is an excellent processing tool for fabrication of high performance components for use in energy conversion and storage devices, which include fuel cells [13], supercapacitors [14] and batteries [15–18]. The numbers of publications, per year, related just to SPS processing of Li-ion batteries/components are also presented as inset of Fig. 1b.

Among the various electrochemical energy storage devices, Li-ion batteries possess significantly higher energy densities and are presently used in a majority of portable electronic devices. Li-ion batteries consist of electrodes, that can reversibly host the charge carrier (Li^+), and electrolytes containing Li-salts in a medium possessing appreciable ionic conductivity [16–33]. Traditionally, liquid electrolytes, such as $LiPF_6$ dissolved in organic solvents, are used in the Li-ion batteries, which consist of graphitic carbon as anode materials and layered oxides (such as $LiCoO_2$ or $LiFePO_4$) as cathode materials [20,21]. A schematic representation of the typical architecture and working principle of Li-ion battery (consisting of liquid electrolyte) is shown in Fig. 2a [33]. Fig. 2b presents a simple schematic of a typical all-solid-state Li-ion battery [34].

The crisis associated with shortage of fossil fuels and necessities for 'green' energy sources have made it imperative to explore the possibilities of using such high performance electrochemical energy storage devices in more heavy duty applications, such as in automobiles. Hence the present focus has been on further improving the energy densities, power densities, cycle lives and safety aspects of such batteries. In this regard, considerable

research efforts are being directed towards the fabrication of dense solid electrolytes [16,19,20,32–41], which provide enhanced safety and design flexibility, nanostructured electrodes [17], which lead to improved power density and cycle lives, and also of entire solid-state Li-ion batteries [18–20]. More recently it has been identified that spark plasma sintering (SPS) offers a facile route towards such otherwise stringent fabrications, bestowing solid electrolytes with improved ionic conductivities and mechanical integrity, electrodes with improved rate capability and the inherently safer all-solid-state batteries with improved energy density, power density and cycle life.

Even though the present world scenario is leading to strong emphasis on the research on materials for energy storage [19–36], it is surprising that, to the best of the author's knowledge, to-date no review article is available in the open literature that summarizes and discusses the advantages offered by spark plasma sintering towards the development of high performance all-solid-state Li-ion batteries. Against this backdrop, the major motivation for this review is to summarize, and hence bring to light in a consolidated manner, some of the promising results that have recently been obtained by using SPS with respect to densifying solid electrolytes and synthesizing nanostructured cathode materials for Li-ion batteries. Such article at this stage is believed to stimulate further research in this area.

Considering that a major fraction of the literature on SPS processed Li-ion battery components focuses on the solid electrolytes, and also since the advantages offered by SPS are probably the most significant for the solid electrolytes, the review will first highlight the necessities for using solid electrolytes, briefly mention the types of solid electrolytes and present a survey detailing the benefits obtained on sintering the ceramic solid electrolytes using SPS. Considering that more recently attempts have also been made to synthesize some of the cathode materials using SPS, a brief survey will also be provided in this respect. Advantages offered by SPS in not only developing the individual components, but also for fabricating the entire solid-state Li-ion batteries will then be looked into. Eventually, a discussion will try to correlate the various improvements achieved in the battery performances with the (micro-) structures obtained down to the atomic levels and with the mechanisms inherent in the SPS process. This discussion will also bring to light the various problems associated with SPS that might be limiting the improvements. The review will conclude by summarizing the promising aspects of SPS with respect to Li-ion batteries, highlighting the grey areas and speculating about further developments possible in the Li-ion battery technology using spark plasma sintering.

2. Solid electrolytes for Li-ion batteries

The ideal electrolyte material would be an electronic insulator, but ionic conductor, ultra-thin, lightweight and safe. Presently commercial lithium ion batteries that use organic liquids as electrolytes have many limitations such as leakage, inflammability and narrow range of operating temperature. Replacing organic liquid electrolytes with solid electrolytes would bring a new perspective to lithium-ion batteries, enabling an intrinsically safe cell design [16,18–20,32–41]. The use of solid electrolyte eliminates the need for containment of the liquid electrolyte, which simplifies the cell design, as well as improves safety and durability. However, solid electrolytes lack in terms of their ionic conductivities, which are sometimes too low to meet the required current density, especially for the more heavy duty applications. Considering that transportation of Li-ions between the electrodes is the primary function of any electrolyte in Li-ion battery, high ionic and interfacial resistances are the major drawbacks for solid electrolytes. Furthermore, the electrolytes need to be stable in ambient atmospheric and operating conditions. It must also be noted that, since structurally the solid electrolytes are at the core of the all-solid-state batteries, the mechanical properties of the solid electrolytes predominantly influence the mechanical integrity of the overall battery. The solid electrolytes can be further classified into two types; viz. polymer electrolytes and ceramic electrolytes.

Typically, polymer electrolytes operate based on two different mechanisms, either via solvation of the lithium salts by the polymer chains {such as with polyethylene oxide (PEO) [37–40]} or via polymer gel formation on the addition of a solvent {such as with poly(vinylidene fluoride) [38–41]}. Block copolymers, such as PEO-b-(PMMA-ran-PMAALi), possessing higher Li-transference number, have also come to the fore in more recent times [42]. Overall, polymers, as solid electrolytes, offer advantages that include facile processability, lesser fabrication costs and enhanced flexibility [36–40]. However, the lower stiffness renders it difficult to use polymer-based electrolytes for batteries requiring greater rigidity. Polymer based electrolytes are also not suitable for use at higher temperatures or under aggressive environments. Another significant drawback of the polymer electrolytes is that they tend to get oxidized in contact with high voltage positive electrodes. Furthermore, poor Li-ion conductivities are another major bottleneck towards the extensive usage of polymer electrolytes.

The other and possibly the more important class of solid electrolytes, allowing still further improved safety for Li-ion batteries, is the ceramic solid electrolyte based on oxides, oxy-nitrides, nitrides, phosphates and sulphides [38,43,44]. Even though some of them are relatively unstable against reduction in contact with metallic Li, especially the oxides and phosphates containing Ti^{4+}, and also lack in terms of Li-ionic conductivities as compared to most liquid electrolytes, being ionic compounds, they are slightly superior in this respect to the polymer based electrolytes (which possess predominantly covalent bonding). Furthermore, ceramic solid electrolyte based batteries are better suited for applications involving higher temperatures, since they are structurally more stable and the ionic conductivity typically increases with increasing temperature. For the applications at ambient temperatures, however, it is imperative to use ceramic electrolytes that possess appreciable room temperature Li-ion conductivities [16,18,19,33–38,43–47]. It must be mentioned here that the Li-ion conductivities of the ceramic electrolytes are strongly influenced by the processing route adopted and the resultant microstructure/interface quality. In this light, the following section will highlight the advantages of using spark plasma sintering to process ceramic based solid electrolytes that are characterized by cleaner interfaces and improved grain-to-grain bonding. Within the scope of this article, the relative differences in the ionic conductivities of the solid electrolytes obtained on processing via SPS, as compared to processing via conventional routes, are of greater significance than the absolute values of such conductivities. Overall, as will be elucidated in the next section, the processing and microstructure play key roles towards their performance and this is where lies the importance of processing via spark plasma sintering, reducing microstructural length scales and engineering interfaces at the atomic levels.

3. Densification, microstructure and ionic conductivities of ceramic electrolytes processed via SPS

One of the ways to improve the ionic conductivities of the ceramic solid electrolytes is by doping them with cations of different valences [16,18,19,33–38,43–49]. In addition to such '*in-situ*' conductivity improvements by changing the chemistry, materials engineering approach can also allow '*ex-situ*' improvement

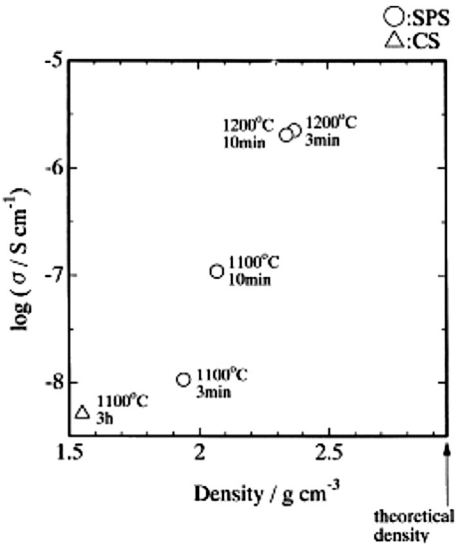

Fig. 3. Ionic Conductivities (at 50 °C) as functions of sinter-densities for undoped phosphate (LTP), processed via spark plasma sintering (SPS) and conventional sintering (CS) [50].

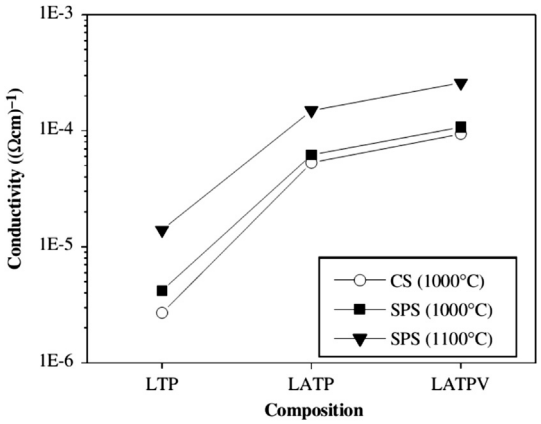

Fig. 4. Ambient temperature ionic conductivities of conventionally sintered (CS) and spark plasma sintered (SPS) $LiTi_2(PO_4)_3$ (LTP), $Li_{1.3}Al_{0.3}Ti_{1.7}(PO4)_3$ (LATP) and $Li_{1.3}Al_{0.3}Ti_{1.7}$ $(PO_4)_{2.9}(VO_4)_{0.1}$ (LATPV) [51].

of the conductivity of the bulk structure used for practical applications [16,18,19,43,44]. Such approach involves reducing the inter-particle/inter-grain porosity, minimizing the microstructural coarsening during porosity removal and achieving clean and 'perfect' interfaces at the sub-nanometre level. Finer and nanosized grains are desirable in ceramic solid electrolytes also from the view point of improving mechanical stability [1,4], which would render such batteries more suitable for applications in automobiles or elsewhere, where the propensity of mechanical/structural damage is higher.

One of the more promising Li^+-ion conductors, which is being considered as one of the potential solid electrolytes in Li-ion batteries is Lithium titanium phosphate (LTP) that has a chemical formula of $LiTi_2(PO_4)_3$ and crystallize in the NASICON (Na-Super-Ionic-Conductor) structure [16,43–53]. They are also stable in air atmosphere. However, the modest ionic conductivity at ambient temperatures of polycrystalline phase pure LTP ($\sim 10^{-7}$ S cm^{-1}) necessitates devising strategies for further enhancement, by at least an order of magnitude, before they can be successfully used as solid electrolytes in Li-ion batteries. One of the ways in which conductivity can be improved is by partial substitution of the Ti^{4+}-ion with trivalent ions such as Al^{3+}, In^{3+} Sc^{3+} [45–49]. Incorporation of other lithium salts, such as Li_3PO_4 and $LiNO_3$, has also been reported to lead to increase in ionic conductivities [46–48].

Irrespective of the changes in composition, processing route and concomitant microstructure/interface engineering also affect the ionic conductivities of LTP. In this perspective, it has been observed by Kobayashi and co-workers [50] that spark plasma sintering leads to two orders of magnitude improvement in the ionic conductivities ($\sim 10^{-6}$ S cm^{-1}) for undoped LTP, with respect to conventional sintering (CS). A comparison between the ionic conductivities obtained with SPS and CS is presented in Fig. 3. Such results show that higher sinter-densities lead to improved ionic conductivities. It must be noted that the ionic conductivities of the conventionally processed LTP [19,20,38,46–48] typically lie in the range, as reported by Kobayashi et al. [50] for the conventionally sintered LTP. A different work by Chang and co-workers [51] also demonstrated that, irrespective of the use of dopants in LTP ceramics, spark plasma sintering leads to enhanced ionic conductivities, which once again scaled with sinter-densities (see Fig. 4). At this stage, comparison of these results seems to suggest that the ionic conductivity of this material, when processed using conventional techniques, is limited mainly by the sinter-density.

As against the observations in these relatively earlier reports, in a very recent work by Duluard et al. [54] it was observed that the conductivity of $Li_{1.3}Al_{0.3}Ti_{1.7}(PO_4)_3$ decreased by nearly an order of magnitude (to $\sim 1 \times 10^{-5}$ S cm^{-1}) on increasing the SPS temperature from 950 °C to 1000 °C, despite leading to slightly higher sinter-density and lower fraction of grain boundaries. Based on SEM observations of the fractured surfaces it was hypothesized that loss of cohesion between grains on sintering at the higher SPS temperature was probably the reason for the significant drop in conductivity. This very recent observation once again emphasizes the importance of good grain-to-grain bonding, which is usually better attained with SPS, albeit under optimized conditions. Hence, even in the case of SPS, optimization of sintering temperature might be important for attaining the best possible ionic conductivities. Further work and analysis need to be done to ascertain if any other mechanistic aspect of SPS processing contributes or does not contribute towards improving the ionic conductivities of LTP. The discussion presented in Section 6 tries to develop a better understanding of these aspects.

Another recent work by Xu et al. [16] provides further information towards developing the correlation between processing, densification, microstructural features and ionic conductivities for $Li_{1.4}Al_{0.4}Ti_{1.6}(PO_4)_3$ (LATP) based solid electrolytes. Spark Plasma Sintering allowed the retention of nanosized grains (<100 nm), while attaining near theoretical densification (see Fig. 5). In fact, negligible particle coarsening/grain growth was observed during SPS of the as-synthesized LATP nanoparticles (~60 nm) at 650 °C. The results, as reported by Xu et al. [16] and Wen et al. [55], are summarized in Table 1 and it can be observed that even though nearly similar sinter-densities were obtained on SPS at 650 °C and 700 °C, the average grain size was lesser by a factor of 2 for the sample sintered (via SPS) at 650 °C. Based on these reports, it seems that such reduction of grain size to nanosized levels, and also further improvement in grain-to-grain bonding, resulted in increment of the grain boundary conductivity by factor of ~1.2 and the total conductivity by a factor of ~1.4. The slightly higher bulk conductivity for the SPS processed LATP, as compared to that conventionally sintered, might also be related to better preservation of the stoichiometry on processing via SPS. Nevertheless, a clear trend of increase in total conductivity with decrease in grain size can be observed from Table 1. More importantly, the total conductivity of the SPS processed sample (at 650 °C) was greater than that of the conventionally sintered sample by a factor of ~3.

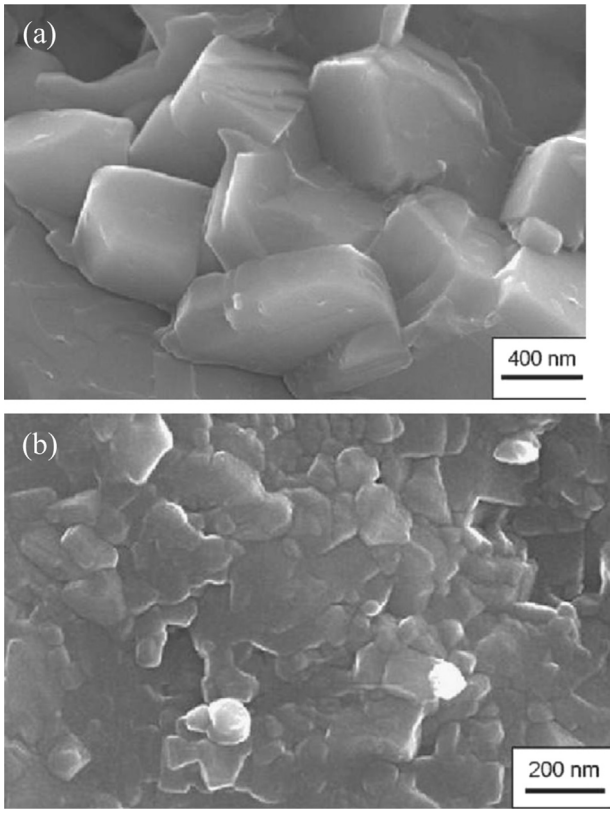

Fig. 5. SEM images of fractured surfaces of $Li_{1.4}Al_{0.4}Ti_{1.6}(PO_4)_3$-based solid electrolytes sintered via (a) conventional sintering technique and (b) spark plasma sintering. Note the presence of nanosized grains in the LATP ceramics sintered via SPS [16].

Interestingly, such results are also supported by the discussion presented in a review paper by Schoonman [56], which reveal that ionic conductivities of solid electrolytes may be improved by nanostructuring.

Replacement of Ti^{4+} with Hf^{4+} is deemed to improve the stability of the NASICON-type solid electrolytes against Li. However, such Hf^{4+} substitution has been associated with poorer densification and phase instability, and concomitantly inferior ionic conductivities [57]. Against this backdrop, Chang et al. [57] reported the attainment of ~75% densification for $LiHf_2(PO_4)_3$ upon spark plasma sintering at 1100 °C for 10 min, which resulted in improvement of the ionic conductivity by more than an order of magnitude, with respect to the conventionally sintered (1100 °C; 2 h) $LiHf_2(PO_4)_3$ (~70% densification). Additionally, combination of spark plasma sintering and Al^{3+} substitution for Hf^{4+} resulted in further improvement of the sinter-density, up to ~90% ρ_{th} (where ρ_{th} stands for theoretical density) for $Li_{1.5}Al_{0.5}Hf_{1.5}(PO_4)_3$, and ionic conductivity, up to 1.1×10^{-4} S cm^{-1}.

On a similar note, with respect to the perovskite based Lithium Lanthanum Titanium Oxides ($Li_{3x}La_{2/3-x}TiO_3$; LLTO), Mei et al. [58] observed considerable increase in the grain boundary conductivity, and hence total conductivity, with increase in sinter-density on varying the SPS temperature between 950 °C and 1050 °C. Even though nearly 98.5% densification was obtained at the SPS temperature of 1050 °C upon holding for 3 min, the total conductivity (~10^{-6} S cm^{-1}) of the LLTO was still found to be limited by the grain boundaries. By contrast, in an earlier work Kobayashi and co-workers [32] had reported the attainment of sinter-densities of ~100% ρ_{th} on spark plasma sintering of LLTO at 1100 °C, with the resultant ionic conductivities being ~10^{-3} S cm^{-1}. At this stage it seems unlikely that the slight difference in sinter-densities would lead to such discrepancy between the ionic conductivities. Rather, this difference in ionic conductivities could possibly be related to the exact stoichiometry (Li-content) of the as-sintered perovskites, which were not mentioned in either of the reports. In this context, it must be mentioned that the ionic conductivity of LLTO is highly dependent on the Li-content and this solid electrolyte is prone to suffering from problems related to Li_2O loss during conventional sintering, which usually requires higher temperatures (>1200 °C) and longer duration (up to 12 h) [59] (as opposed to between 3 and 5 min via SPS [32,58]).

With respect to garnet-type solid electrolytes, such as $Li_5La_3Bi_2O_{12}$, spark plasma sintering resulted in attaining better densification (~97% ρ_{th}) of nanosized powders, synthesized by Pechini method, at a lower temperature of 923 K [60] (~200 K lower compared to conventional sintering [61,62]) and shorter time of 5 min (as against 5 h for conventional sintering). Improved sinter-density and better control of stoichiometry in SPS led to the attainment of improved total conductivity of $\sim 5.1 \times 10^{-5}$ S cm^{-1} [60], which was higher by a factor of 2 compared to that achieved for $Li_5La_3Bi_2O_{12}$, sintered via conventional sintering [61,62]. In addition to phosphate and oxide based electrolytes, Liu et al. [63] reported an order of magnitude improvement in room temperature ionic conductivities, along with reduction in activation energies, on spark plasma sintering of sulphide based novel Li_4SiS_4–La_2S_3 composite solid electrolytes. This one order of magnitude improvement was with respect to cold pressed electrolytes of similar composition, whereas the overall improvement obtained with respect to the more conventional and unreinforced Li_4SiS_4 was ~4 orders of magnitude.

Table 2 provides a summary of the ionic conductivities recorded with the various ceramic solid electrolytes, densified using spark plasma sintering to-date. Corresponding data from those sintered via conventional route are also included. These emphasize the role of advanced sintering techniques like spark plasma sintering in

Table 1
Correlation between sinter-densities (as % of theoretical densities; % ρ_{th}), grain size and room temperature ionic conductivities (bulk, grain boundary and total) for the two more commonly investigated ceramic solid electrolytes; viz. $Li_{1.4}Al_{0.4}Ti_{1.6}(PO_4)_3$ (LATP) [16,55] [processed via conventional solid state sintering (CSSS), crystallization from glass (GC) and spark plasma sintering (SPS)] and $Li_{3x}La_{2/3-3x}TiO_3$ (LLTO) [processed via SPS] [32,58].

Processing techniques and conditions	Average grain size (nm)	Sinter-density (% ρ_{th})	Bulk conductivity (S cm^{-1})	Grain boundary conductivity (S cm^{-1})	Total conductivity (S cm^{-1})	Reference
$Li_{1.4}Al_{0.4}Ti_{1.6}(PO_4)_3$ (LATP)						
SPS at 650 °C	<100	~100.0	~3.25×10^{-3}	~1.39×10^{-3}	~1.12×10^{-3}	[16,55]
SPS at 700 °C	~300	~99.0	~3.17×10^{-3}	~1.02×10^{-3}	~0.78×10^{-3}	[16,45]
GC at 950 °C	~600	~97.0	–	~0.93×10^{-3}	~0.49×10^{-3}	[55]
CSSS at 850 °C	~1000	~95.0	~3.01×10^{-3}	~0.79×10^{-3}	~0.36×10^{-3}	[16,55]
$Li_{3x}La_{2/3-3x}TiO_3$ (LLTO)						
SPS at 950 °C	~2000	~93	~1.25×10^{-3}	~2.0×10^{-6}	–	[58]
SPS at 1000 °C	~2000	~97	~1.30×10^{-3}	~3250×10^{-6}	–	[58]
SPS at 1050 °C	~2000	~98.5	~1.30×10^{-3}	~5750×10^{-6}	~5.8×10^{-6}	[58]
SPS at 1100 °C	–	~100	–	–	~1.0×10^{-3}	[32]

Table 2
Summary of the ionic conductivities of the various ceramic solid electrolytes, sintered via SPS. Data for the conventionally sintered (CS) solid electrolytes are also provided for comparison. Note that data from same work has been grouped together.

Materials	Processing techniques and conditions	Total conductivity (S cm^{-1})	Reference
$LiHf_2(PO_4)_3$	SPS at 1100 °C	2.6×10^{-5}	[57]
	CS at 1100 °C	6.5×10^{-6}	
	CS at 1000 °C - 1100 °C	3.0×10^{-6}	[53]
$Li_{1.5}Al_{0.5}Hf_{1.5}(PO4)_3$	SPS at 1100 °C	1.1×10^{-4}	[57]
$LiTi_2(PO_4)_3$	SPS at 1100 °C	1.4×10^{-5}	[51]
	CS at 1000 °C	2.7×10^{-6}	
	SPS at 1200 °C	10^{-6}	[50]
	SPS at 1100 °C	10^{-7}	
	CS at 1100 °C	10^{-8}	
	CS at 900 °C–1250 °C	2.0×10^{-6}	[46]
$Li_{1.3}Al_{0.3}Ti_{1.7}(PO_4)_3$	SPS at 950 °C	1.6×10^{-4}	[54]
	SPS at 1100 °C	2.0×10^{-4}	[51]
	CS at 1000 °C	0.5×10^{-5}	
$Li_{1.3}Al_{0.3}Ti_{1.7}(PO_4)_{2.9}(VO_4)_{0.1}$	SPS at 1100 °C	2.6×10^{-4}	[51]
	CS at 1000 °C	0.8×10^{-5}	
$Li_5La_3Bi_2O_{12}$	SPS at 650 °C	5.1×10^{-5}	[60]
	CS at 750 °C	1.9×10^{-5}	[61]
$Li_6SrLa_2Bi_2O_{12}$	SPS at 650 °C	6.8×10^{-5}	[60]
	CS at 750 °C	2.0×10^{-5}	[61]
$(Li,La)TiO_3$	SPS at 1100 °C and 1200 °C	1×10^{-3}	[32]
	CS at 1200 °C	1×10^{-3} (bulk)	[59]
Li_4SiS_4–La_2S_3	SPS at 400 °C	1.2×10^{-4}	[63]
	Treated at 750 °C	3.0×10^{-5}	[63]

improving the performance of solid electrolytes used in Li-ion batteries. It must be mentioned here that the interfacial ionic conductivities of such ionic conductors, which can be anomalous in nature, are governed by a field called 'nanoionics' [64], more detailed discussion on which is beyond the scope of the present paper.

4. Synthesis of cathode materials using SPS

Since improvement of power density is one of the primary requirements for rendering Li-ion batteries suitable for use in heavy duty applications, nanostructuring of electrode materials, leading to enhanced rate capabilities, has been one of the major research focuses over the last decade. The more widely used solid-state synthesis for synthesizing cathode materials typically involves high temperature exposure for elongated duration. This results in coarsening of the cathode particles, and hence deterioration of the rate capabilities. Such elevated temperature exposure induced coarsening, coupled with the intrinsically poor electronic and ionic conductivities of the ceramic cathode materials (such as $LiFePO_4$; possessing higher theoretical Li-capacity ~170 mA h g^{-1} [65–69]), necessitates the use of processing route that would allow synthesis of nanosized cathode particles. It must be noted here that in the case of cathode materials, SPS technique has primarily been used for improved synthesis and treatment, rather than for densification.

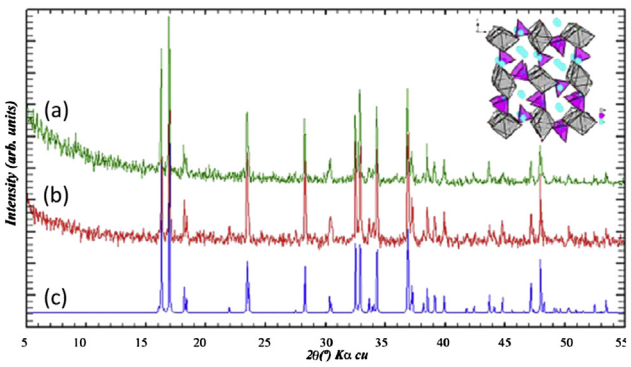

Fig. 6. X-ray diffraction patterns of Li_2CoPO_4F (a) processed via SPS; (b) processed following conventional synthesis route; and (c) calculated using JCPDS 56-1493 [17].

Among the more recently investigated cathode materials, fluorophosphates like Li_2CoPO_4F possess appreciable theoretical Li-capacity [17,70]. However, similar to the case of the more conventional cathode materials such as $LiFePO_4$, the fluorophosphates lack in terms of their rate capability. This problem gets accrued for particles of larger sizes, which is often the case on synthesis by conventional solid-state routes. In order to address this issue, very recently Botto et al. [17] attempted the synthesis of Li_2CoPO_4F from stoichiometric mixtures of $LiCoPO_4$ and LiF via spark plasma sintering. As can be seen from Fig. 6, stoichiometric Li_2CoPO_4F, possessing orthorhombic crystal structure (Pnma) could be synthesized via SPS. More importantly, the synthesis was completed within 9 min at 700 °C, as opposed to 10 h required during conventional synthesis. Such significant reduction in processing time led to the successful formation of Li_2CoPO_4F nanoparticles via SPS, as against the coarser micron-sized particles when synthesized using the conventional route (see Fig. 7). In a very recent work, Arachi et al. [71] has reported the possibility of obtaining dense and phase pure $Li_{2-x}FeSi_{1-x}P_xO_4$ based novel cathode materials, with minimum carbon content (<3 wt.%), possessing significantly improved ionic and electronic conductivities, within few minutes of SPS treatment starting with mixed precursor compounds. On a similar note, work by Galy et al. [9] has revealed that it is possible to synthesize Vanadium oxide bronzes ($M_xV_2O_5$; M = Cu or Ag) with controlled stoichiometry, directly from mixtures of V_2O_5 and M powders, within few minutes using SPS. Such synthesis via conventional solid-state route usually takes significantly longer time (even up to couple of days), and is one of the bottlenecks towards practical application of these otherwise higher capacity cathode materials (capacity ~315 mA h g^{-1} [72]).

Introduction of conducting additives, such as carbon, to the insulating cathode particles has also been deemed to be one of the ways for improving the conductivity of the cathode particles. In this respect, coating with carbon films of thickness preferably in the nanosized regime is a better strategy as compared to adding the conductive fillers [35,73]. However, good bonding at the atomic

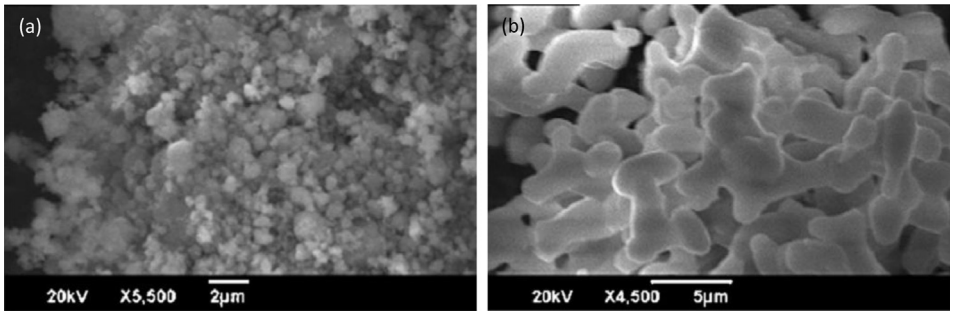

Fig. 7. Scanning electron micrographs of (a) synthesized via SPS and ball milled; (b) conventionally synthesized and ball milled Li_2CoPO_4F cathode particles [17].

level between the insulating cathode particles and the conducting carbon coating is essential to result in the improved performance. In fact, improved rate capabilities and cyclic performances have been observed for oxide [18,34,74–76], as well as metal-sulphide [77,78], based cathode materials, when the cathode/C composites were processed using spark plasma sintering.

With respect to the more common cathode material ($LiCoO_2$), it could be clearly observed from the work of Takahara et al. [34] that SPS treatment of a mixture of $LiCoO_2$ and acetylene black resulted in considerably improved specific capacity (by factor of ~1.5), as compared to the untreated mixture, for the same carbon content (2.5 wt.%) and at the same current density (0.32 mA cm^{-2}). Further improvement in the capacity (by factor of ~2) was obtained on having the $LiCoO_2$ particle surfaces coated with carbon films *in-situ* during SPS treatment. It was also noted that the improvements were more pronounced at the higher current density (see Fig. 8a), implying that SPS treatment is particularly helpful for attaining superior rate capabilities. Few years later, the same Japanese group, in collaboration with couple of other groups, reported similar observations with $LiNi_{0.8}Co_{0.15}Al_{0.05}O_2$/C composite cathode materials [74]. In this subsequent work [74], an additional step of first treating the acetylene black (AB) using SPS to form high density acetylene black (HDAB) was followed by treating the $LiNi_{0.8}Co_{0.15}Al_{0.05}O_2$/

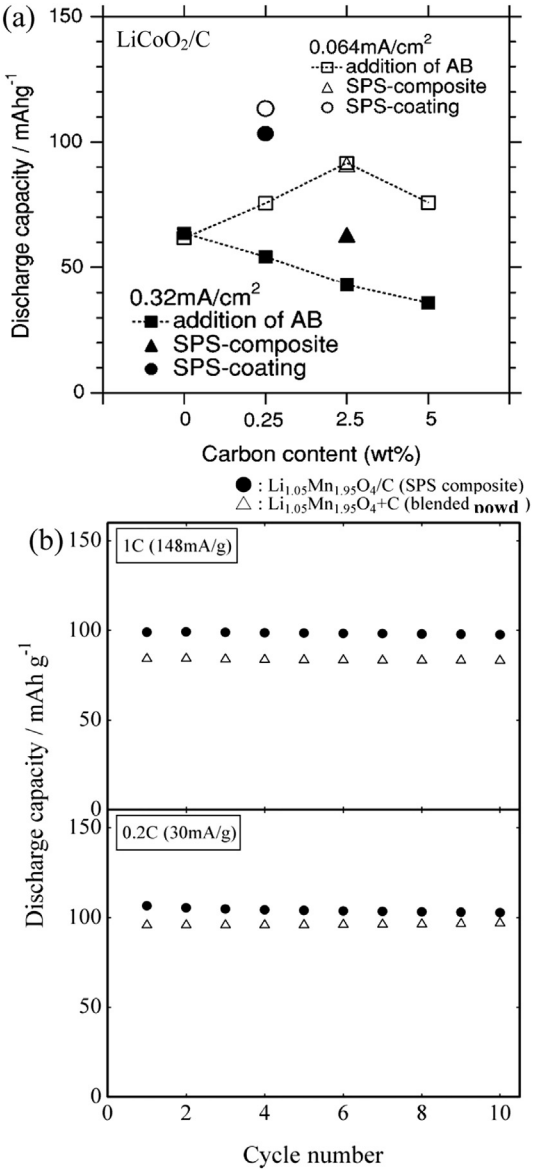

Fig. 8. Cyclic behaviour for (a) $LiCoO_2$/C [34] and (b) $Li_{1.05}Mn_{1.95}O_4$/C composites [75] (mixed/blended powder and SPS processed) at different current densities. Note the considerably improved rate capability for the SPS processed composites.

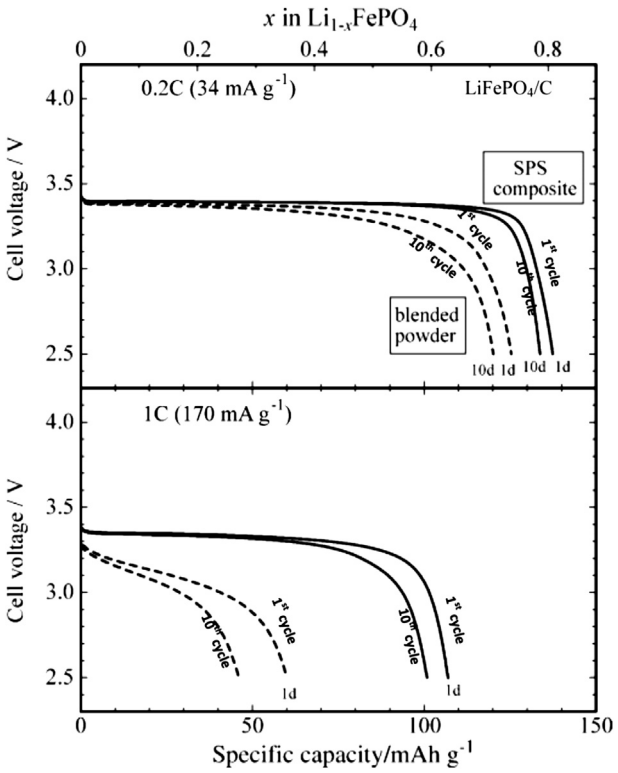

Fig. 9. Effects of SPS treatment on the improvements of specific capacity and rate capability of $LiFePO_4$/C cathode material [76].

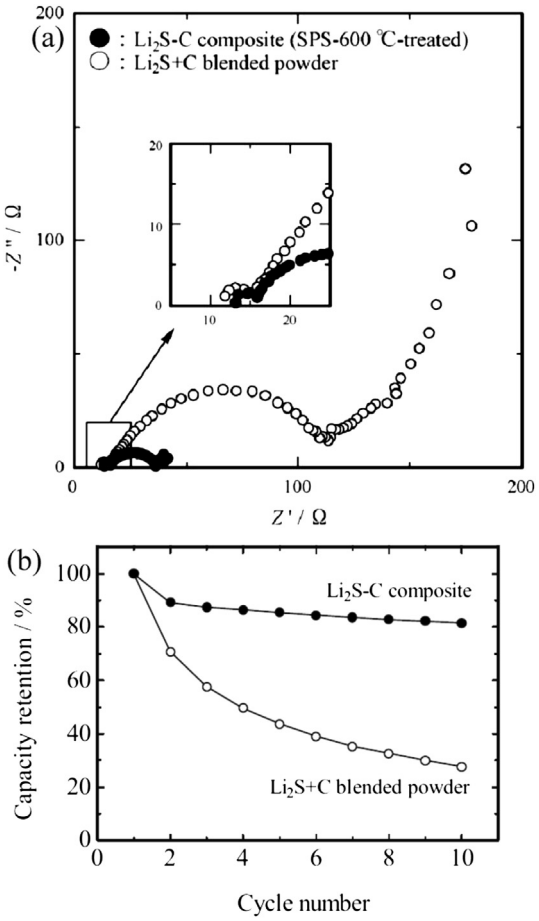

Fig. 10. Comparison of (a) Nyquist plots (after full charging) and (b) capacity retention (as % of capacity in 1st cycle) obtained with SPS treated (600 °C) and conventionally blended Li_2S + C electrodes [77,78].

HDAB mixture using SPS. This two-step SPS treatment led to the increase in the volumetric capacity by nearly factor of 1.25, along with improved rate capability and cycle life, with respect to the blended $LiNi_{0.8}Co_{0.15}Al_{0.05}O_2$/AB.

For the spinel-based cathode material, viz. $Li_{1.05}Mn_{1.95}O_4$/C, SPS treatment of the mixture, containing 10 wt.% carbon, at just 300 °C for 5 min was observed to lead to improved capacity retention at the higher electrochemical cycling rate, as can be seen in Fig. 8b [75]. Similarly, for the olivine based cathode material, viz. $LiFePO_4$/C, SPS treatment at 600 °C resulted in considerably improved rate capability and capacity retention upon cycling (see Fig. 9), with respect to the blended mixture [76]. These were mainly attributed to the formation of stronger bonding between the carbon and $LiFePO_4$ upon SPS treatment. Furthermore, reducing conditions prevailing during SPS resulted in lowering of the Fe^{3+}-containing phase in $LiFePO_4$, which in turn led to improved specific capacity.

The use of SPS has been found to be even more beneficial for Li_2S/C [77–79], which are considered as the next generation cathode materials due to their significantly higher specific capacity (~1170 mA h g^{-1}). As reported by Takeuchi et al. [77], good bonding between Li_2S and C attained during SPS treatment (at ~600 °C) significantly reduces the interfacial resistance (see Fig. 10a) with respect to conventionally blended powder and allows better utilization of the active material. Such improved Li_2S/C interface of the SPS treated composite resulted in attaining specific capacities up to near theoretical capacity when cycled against Li/Li^+ in a suitable electrolyte solution, whereas negligible capacities were recorded with conventionally blended powders, as also in other works [77–79]. The superior capacity retention of the SPS treated Li_2S/C composite, as compared to the blended powder, is also shown in Fig. 10b [77]. On a slightly different note, for the composite cathode materials, simultaneous densification during SPS treatment also results in improved tap density, leading to overall greater volumetric energy density [74,75,78].

5. Fabrication of solid-state Li-ion batteries using SPS

As has been stated earlier, all-solid-state Li-ion batteries are beneficial in terms of safety and durability, especially for the more advanced and heavy duty applications [16,18,19,31–41]. However, the resistances at the interfaces between the solid electrolytes and the electrodes are the major bottlenecks towards the functioning of such devices. Such accrued resistances can result from the formation of 'unclean' and less perfect interfaces on sintering of stacked electrode/electrolyte pellets via conventional techniques. Against this backdrop, Kobayashi and co-workers [50] fabricated stacked pellets of $LiTi_2(PO_4)_3$/$LiCoO_2$ (i.e. solid electrolyte/cathode) via spark plasma sintering. It is believed that the cleaner interface with improved bonding, that formed between $LiTi_2(PO_4)_3$/$LiCoO_2$ during SPS, possessed lesser resistance and better mechanical integrity as compared to those produced via conventional sintering. This opened up the possibilities for fabrication of all-solid-state Li-ion batteries, possessing improved transport properties and mechanical stability of the interface. However, characterization at the sub-nanometre level, leading to better understanding of the interface structure was not presented in the work by Kobayashi et al. [50].

In a more recent work, Aboulaich et al. [18] fabricated all-solid-state inorganic Li-ion batteries via spark plasma sintering. $Li_{1.5}Al_{0.5}Ge_{1.5}(PO_4)_3$ (LAG) glass ceramic was selected as the solid electrolyte, $LiFePO_4$ (LFP) as the cathode active material and $Li_3V_2(PO_4)$ (LVP) as the anode active material. In order to ensure

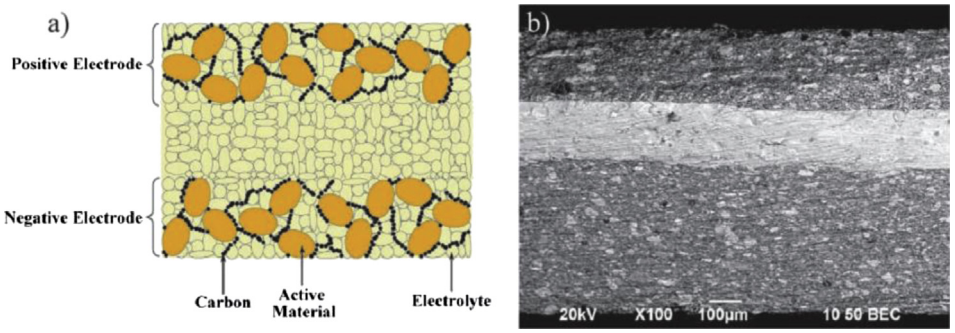

Fig. 11. (a) Schematic representation and (b) cross-sectional SEM image of the all-solid-state Li-ion battery fabricated via spark plasma sintering, showing the three layers (LFP – C/LAG/LVP – C) [18].

good electrical conductivities for the cathode and anode, which are inherently insulators, conductive additive in the form of carbon black was added. Spark plasma sintering of the stacked laminates at 680 °C for 10 min resulted in the fabrication of self-supported multilayered pellets (LFP-C/LAG/LVP-C) possessing good mechanical integrity. SEM image and schematic representation of the stacked assembly are shown are Fig. 11. It must be mentioned here that conventional sintering of such stacked pellets usually results in the cracking of the interfaces due to thermal stresses. Detailed HRTEM observations revealed the formation of atomically clean and 'perfect' interfaces between the electrode active material/carbon additive and the electrode/electrolyte (see Fig. 12a and b). TEM observations also confirm the retention of the grain sizes of $LiFePO_4$ in the nanosized regime after spark plasma sintering (Fig. 12c). Such nanostructured electrode active materials, atomically clean/well-connected interfaces and mechanically stable structures would lead to superior power densities and cycle lives for the all-solid-state Li-ion batteries, as demonstrated by the electrochemical results obtained with the as-fabricated LFP-C/LAG/LVP-C cell. We believe that replacement of the carbon additives in all-solid-state batteries with carbon nanomaterials such as nanofibres or nanotubes would be feasible since, unlike other sintering techniques, SPS would preserve the integrity of the nanomaterials and the interfaces, thus leading to even superior power densities.

6. Correlation between the mechanistic aspects of SPS and relevant property enhancement

The various mechanisms involved in SPS and the corresponding mathematical models have been elucidated time and again in various review articles [1–5]. The effects of processing via SPS on the properties of the solid electrolytes, electrodes and all-solid-state Li-ion batteries have formed the basis of the discussion in the preceding sections of this review article. With respect to the solid electrolytes, the important advantage of using SPS is the improvements obtained with the net ionic conductivity; most of the research results related to which have been highlighted in this review (see Section 3 and Tables 1 and 2). A majority of the articles [16,18,19,50,51,54–63] concerned with the sintering of solid electrolytes via SPS tends to associate the improved sinter-densities, and sometimes the finer grain sizes also, with the improved ionic conductivities. Few researchers [18] have also taken a closer look at the grain boundaries/interfaces of the SPS processed ceramic electrolytes and have reported the presence of atomically clean grain boundaries. It must be mentioned here that the actual reason(s) for the significant improvements in the performance of the solid electrolytes, electrodes and all-solid-state Li-ion batteries on processing via SPS still remain to be established unambiguously.

The basic theory governing the phenomenon of ionic conduction in polycrystalline ceramics would shed some light into this grey area. Usually some of the defects present in the polycrystalline ceramics, such as grain boundaries and porosities, lead to decrease in the overall ionic conductivities. In fact, grain boundary conductivities can be an order of magnitude lower as compared to the bulk conductivities. Various factors affect the grain boundary conductivities, which include disorder, presence of impurities, presence of porosities and inefficient grain-to-grain bonding at the boundaries of the polycrystalline ceramics sintered from powder compacts. Based on this, it can be envisaged that lesser the volume fraction of grain boundaries and porosities, the better it is for the overall ionic

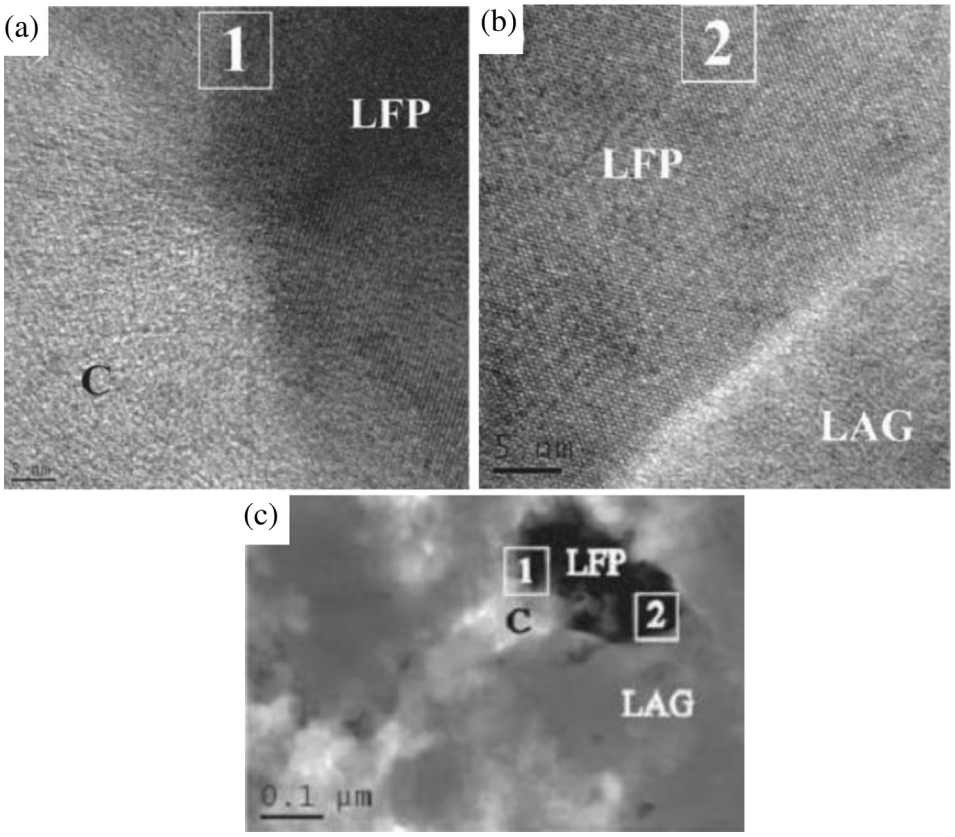

Fig. 12. HRTEM images showing atomically clean interfaces and good connections between (a) cathode active $LiFePO_4$ (LFP) particle and conducting additive (carbon; C) and (b) LFP and $Li_3V_2(PO_4)$ (LVP) solid electrolyte for the all -solid-state Li-ion battery fabricated via SPS. Note that the images were captured after 30 discharge/charge cycles, which points towards the mechanical integrity of the interfaces. (c) TEM image showing the retention of nanosized grains of LFP after spark plasma sintering [18].

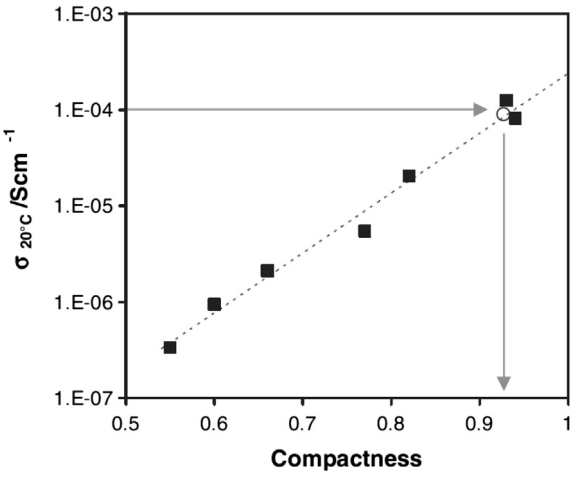

Fig. 13. Variation of conductivity of $Li_{1.5}Al_{0.5}Ge_{1.5}(PO_4)_3$, sintered via SPS, as a function of compactness (sinter-density) [35].

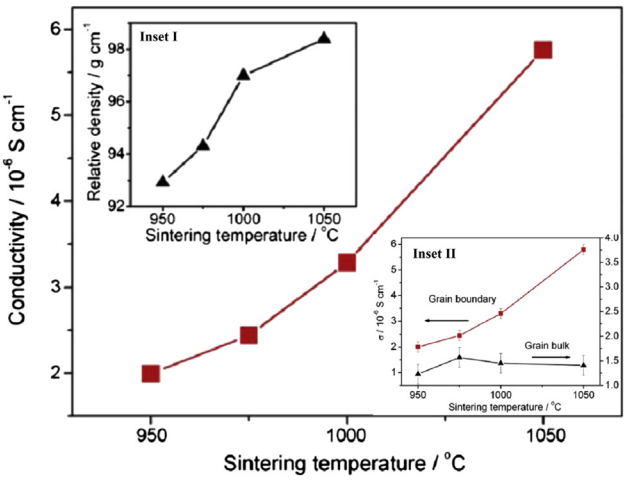

Fig. 14. Plots showing the correlation between total conductivity (main plot), sinter-density (inset I) and de-convoluted bulk and grain boundary conductivities (inset II) with spark plasma sintering temperature for Lithium Lanthanum Titanium Oxide based solid electrolyte for Li-ion batteries. [58].

conductivities. However, from few published results [16,55] and also Table 2 it can be observed that solid electrolytes processed via SPS often possess finer grain sizes (and hence higher volume fraction of grain boundaries) and yet possess higher ionic conductivities than their conventionally sintered counterparts. Even though the actual effect of grain size on the ionic conductivities of solid electrolytes is still a grey area, the preceding discussion points to the possibility of a combination of some other factors playing a significant role towards counterbalancing the expected negative influence of increase in volume fraction of grain boundaries (due to grain size reduction) on processing via SPS.

The reduction in the volume fraction of porosities due to slightly better densification achieved via SPS is easily one of the factors contributing towards the improvement in the overall ionic conductivities. With respect to the basic mechanisms leading to higher sinter-densities using SPS, it is believed that faster heating rates and enhanced mass transport, possibly due to plasma generation between the powder particles or electro-migration [1–5], as well as the minimization of particle coarsening, all contribute together. Good correlations between improvements in sinter-densities and ionic conductivities have been reported by many researchers [50,51,60–63]. In particular, in a very recent work, Delaizir et al. [35] has reported that the room temperature ionic conductivity can decrease by a factor of ~6.4 with every 10% decrease in the sinter-density for $Li_{1.5}Al_{0.5}Ge_{1.5}(PO_4)_3$, sintered via SPS (Fig. 13). It was suggested that at least 80% densification would be needed for attaining reasonable ionic conductivities (~10^{-5} S cm^{-1}) that would allow the ceramic material to be used as solid electrolyte at near room temperatures.

On a similar note, with respect to the spark plasma sintered LLTO solid electrolytes, Mei et al. [58] had clearly demonstrated that the overall ionic conductivity varies in the same way with SPS temperature as sinter-density (see Fig. 14 and Table 1). Deconvolution of the overall conductivity into bulk and grain boundary components revealed that it is the grain boundary conductivity which increases with increasing SPS temperature in accordance to the sinter-density, whereas the bulk conductivity remains virtually unchanged (see inset II of Fig. 14). Furthermore, Liu et al. [63] had observed that spark plasma sintering of novel Li_4SiS_4–La_2S_3 composite solid electrolytes results in improvement in the density by a factor of ~1.5 with respect to cold pressed electrolytes of the same composition. This superior density was deemed to be the major reason for the one order of magnitude higher ionic conductivity obtained on spark plasma sintering. Based on the absence of the higher frequency semi-circle in the impedance spectra of the spark plasma sintered solid electrolytes, but with negligible difference in the lower frequency spikes with respect to the cold pressed electrolytes, it was also hypothesized that the improvement in ionic conductivity upon spark plasma sintering stems mainly from the decrease in grain boundary resistance, which was in turn the result of improved grain-to-grain bonding (or higher sinter-density). This hypothesis is also in accordance with the results obtained by Mei et al. [58] for LLTO. However, closer look at some other results might indicate still some ambiguity with respect to the correlation between sinter-densities and ionic conductivities for the solid electrolytes. For instance, in the more recent work, Duluard et al. [54] observed drastic fall in net conductivity (by an order of magnitude) of LATP on increasing the SPS temperature from 950 °C to 1000 °C, even though sinter-density increased slightly.

Based on the published literature [1–6] on spark plasma sintering it is believed that the films on the powder particle surfaces break down (dielectric break down) and spark discharge takes place between the powder particles during the initial stages. Unlike in the conventional sintering processes, such phenomena during the initial stages of SPS clean the surfaces of the powder particles. When the powder surfaces get bonded during the eventual sintering processes forming grain boundaries, good grain-to-grain bonding and atomically clean grain boundaries are achieved. This has been evidenced with various polycrystalline ceramic materials, including solid electrolytes, by direct observation using high resolution TEM [1,18,80]. Additionally, shorter processing times involved with SPS would also possibly minimize/prevent formation of deleterious grain boundary phases from unwanted sintering reactions. Such 'superior' grain boundaries, as formed on processing via SPS, should ideally lead to higher ionic conductivities. This has indeed been observed on de-convoluting the overall conductivities into bulk and grain boundary contributions for some of the solid electrolytes, as has also been mentioned earlier and reported in Table 1. Additionally, the same mechanisms also render SPS beneficial for the development of all-solid-state batteries, with lower resistances across the various interfaces (see Section 5). The cleaning action and shorter duration of SPS can also lead to the better preservation of stoichiometry and lowering of impurity content, which possibly can improve the bulk conductivity as well, which was observed in the work of Xu et al. [16] (see Table 1).

Even though, in this review, the minimization of particle coarsening/grain growth during processing via SPS has not been

considered particularly beneficial towards solid electrolytes, it is this phenomenon which assumes importance during synthesis of finer sized (up to nanoscaled dimensions) cathode particles via SPS. Once again, the faster heating rates, which allow reaching the synthesis temperature much sooner, and enhanced mass transport, which allows completion of synthesis in significantly shorter duration, enables the retention of finer particles. It must be mentioned here that the lower synthesis temperature, as is typically quoted for SPS, might also be dependent on the technique used for the temperature measurement [1,6].

At this stage, even though most of the improvements in ionic conductivities obtained on processing via SPS can be qualitatively explained based on the twin theories of reduction of residual porosities and formation of 'superior' grain boundaries, while the improved performances of the cathodes are related to faster heating rates and mass transport during SPS, some of the more ambiguous observations, including that of Duluard et al.'s [54], still indicate possible interplay between other factors. Effects of SPS processing on stoichiometry, possible grain boundary segregations and occurrences of sintering reactions under different SPS conditions need to be considered for more comprehensive understanding of the phenomenon and for bringing to light some possible issues that might be associated with SPS processing of battery components.

For instance, Takahara et al. [34] observed that SPS treatment beyond 400 °C within the graphitic carbon die usually leads to partial decomposition of $LiCoO_2$, forming CoO and Co_3O_4. Interestingly, the electrochemical results (see Fig. 8a) suggest that the advantages offered by the SPS treatment, in terms of good interfacial bonding, may possibly circumvent the problem related to partial dissociation. Looking beyond the solid electrolytes that are used in Li-ion batteries, spark plasma sintering of Na-based NASICON ceramics, such as $Na_3Zr_2Si_2PO_{12}$, allowed attainment of sinter-densities, and hence Na^+ conductivities, that were superior to the conventionally sintered $Na_3Zr_2Si_2PO_{12}$ ceramics [81]. However, with respect to phase stability, presence of ZrO_2, possibly due to volatilization of Na and P during SPS, was observed in the SPS processed $Na_3Zr_2Si_2PO_{12}$, as opposed to the phase pure NASICON prepared by conventional sintering. It is possible that such enhanced volatilization induced decomposition/phase instability during SPS might also be affecting the performance of the more relevant NASICON type solid electrolytes for Li-ion batteries, such as $LiTi_2(PO_4)_3$ (see Sections 2 and 3), and in fact might also be one of the possible causes for the anomalous results obtained by Duluard et al. [54], as discussed earlier. In this context, in a very recent report, though not related to the fabrication of battery components, the author [6] has elucidated the possibilities of phase instabilities during sintering via SPS due to enhanced mas transport inherent in the SPS process. However, if properly investigated [58], such non-stoichiometry/phase instability of the SPS processed component can be prevented by carefully adjusting the composition of the starting powder. Such detailed investigation, even just related to the extent of possible loss of Li due to vaporization during spark plasma sintering of Li-containing electrolytes/electrodes, has not been performed in majority of the reported research.

With respect to Li-loss during SPS, Mei et al. [58] has reported some loss of Li from the grain boundaries of LLTO, but has claimed that the losses are much less significant compared to those during conventional sintering which requires longer duration. Similarly, Gao et al. [60] also mentioned about the possibility of better control of stoichiometry, due to lesser volatilization induced loss of Li and Bi-based components, during SPS of $Li_{5+x}Sr_xLa_{3-x}Bi_2O_{12}$ based electrolytes. These are, however, in contrast to Lee et al.'s [81] observation of accrued loss of Na^+ during spark plasma sintering of $Na_3Zr_2Si_2PO_{12}$. On a slightly different note, none of the studies to-date has also taken into consideration the effects of possible contamination by carbon, since SPS is performed typically on powders contained in a graphite die. These issues definitely warrant more extensive and detailed investigations.

7. Conclusion and outlook

The feasibilities of fabricating high performance solid electrolytes, electrode materials and entire solid-state Li-ion batteries using spark plasma sintering, and the mechanistic aspects of SPS that allow such developments, have been demonstrated in this review article. SPS contributes towards alleviating, to a significant extent, the major drawbacks of solid electrolytes, which arise from their intrinsically poor ionic conductivities. Attainment of good sinter-densities and formation of atomically clean grain boundaries with good grain-to-grain bonding result in improved ionic conductivities and better mechanical properties for the ceramic solid electrolytes sintered via SPS. Synthesis of the cathode materials using SPS has also been observed to be beneficial in terms of the rate capabilities, which is primarily due to minimization of particle coarsening and formation of stronger bonding between cathode active particles and conducting additives during synthesis via SPS. In addition to the development of electrolytes and electrodes, SPS has opened up possibilities to successfully fabricate the entire solid-state Li-ion battery by sintering of stacked ceramic layers for few minutes. As opposed to conventional sintering, SPS leads to the formation of nearly 'perfect' and mechanically stable interfaces between the electrodes and the electrolyte. This, along with the advantages mentioned above for electrodes and solid electrolytes, allow the fabrication of mechanically stable batteries with lower internal resistances, improved rate capabilities and overall higher power densities.

It must be mentioned here that the use of SPS for fabricating Li-ion batteries is an upcoming area and is yet to be explored to the maximum possible potency. We believe that with more rigorous optimization of the composition and processing conditions, synthesis via SPS would allow solving the inherent problems of lower rate capabilities of most of the ceramic electrode materials. Also, multi-stage spark plasma sintering (MSS-SPS), which is a very recent innovation based on the regular SPS route by the author and co-workers [7,82,83], and which improves the microstructural homogeneity of the sintered component, is yet to be applied towards the development of solid electrolytes and solid-state batteries. Similarly, understanding of the possible improvements of the mechanical integrity of electrolytes and entire battery on processing via SPS is yet to be investigated and is still another totally open area for research.

As pointed out in the previous section, more detailed investigation is needed to get a better insight into the issues concerning phase stability, volatile loss of Li^+ and possible contamination during SPS. On a different note, since the dimensions of SPS processed all-solid-state batteries are usually governed (restricted) by the sizes of the dies, the scalability of the fabrication via SPS to the commercial level needs to be given due consideration. Furthermore, extensive work is needed to develop better control over the exact dimensions (in particular, thickness) of the batteries fabricated via SPS, which might be necessary for possible integration with electronic devices.

With respect to the more commonly investigated transport properties, SPS might bestow still further improved transport properties to some of the more recently introduced and extremely promising solid electrolytes, such as $Li_{10}GeP_2S_{12}$ [36,84] that possess one of the highest reported room temperature ionic conductivities of $\sim 10^{-2}$ S cm^{-1}. This could also be true for the various glassy solid electrolytes, such as Li_2S–SiS_2–Li_3PO_4 [85], which

possess appreciable ionic conductivities of $\sim 10^{-3}$ S cm^{-1} even on being processed via conventional techniques. As has been described in the preceding sections, attempts have been made to process a majority of the ceramic solid electrolytes and many cathode materials via SPS. However, we believe that the inert (and slightly reducing) atmosphere and faster processing time of SPS should be particularly beneficial for these sulphides, which are known to be hygroscopic in nature. Also, with respect to the atmosphere, investigation and understanding of the effects of the SPS atmosphere on the oxidation state of the transition metals in the oxide and phosphate based solid electrolytes/cathodes is another grey area. In addition to such possible improvements in properties, it is also believed that synthesis via SPS might open up vistas for developing electrodes and solid electrolytes based on different nanocomposite/nanostructured materials that have not been feasible to-date using the more conventional processing techniques. In this respect, the advantages of SPS in terms of preserving the initial dimensions, stoichiometry and structural integrity can be exploited for fabricating electrodes, electrolytes and all-solid-state batteries using various nanomaterials, such as nanoparticles, nanorods and nanotubes.

References

[1] A. Mukhopadhyay, B. Basu, Intl. Mater. Rev. 52 (5) (2007) 257–288.
[2] M. Omori, Mater. Sci. Eng. A 287 (2) (2000) 183–188.
[3] J.R. Groza, A. Zavaliangos, Mater. Sci. Eng. A 287 (2) (2000) 171–177.
[4] M. Nygren, Z. Shen, Solid State Sci. 5 (2003) 125–131.
[5] R. Orru, R. Licheri, A.M. Locci, A. Cincotti, G. Cao, Mater. Sci. Eng. R 63 (2009) 127–287.
[6] A. Mukhopadhyay, T. Venkateswaran, B. Basu, Scr. Mater. 69 (2) (2013) 159–164.
[7] D. Jain, K.M. Reddy, A. Mukhopadhyay, B. Basu, Mater. Sci. Eng. A 528 (1) (2010) 200–207.
[8] A. Mukhopadhyay, G.B. Raju, B. Basu, in: I.M. Low, Y. Sakka, C.F. Hu (Eds.), Max Phases and Ultra-high Temperature Ceramics for Extreme Environments, IGI Global, Hershey, 2013, pp. 49–99.
[9] J. Galy, M. Dolle, T. Hungria, P. Rozier, J. -Ph. Monchoux, Solid State Sci. 10 (8) (2008) 976–981.
[10] A.G. Bloxam, GB Patent, No. 27,002 and GB Patent, No. 9020, 1906.
[11] K. Inoue, U.S. Patent No. 3241956, 1962.
[12] G. Xie, J. Powder Metall. Min. 2 (2) (2013) 1–3.
[13] T. Mori, T. Kobayashi, Y. Wang, J. Drennan, T. Nishimura, J.-G. Li, H. Kobayashi, J. Am. Ceram. Soc. 88 (7) (2005) 1981–1984.
[14] B. Daffos, G. Chevallier, C. Estournès, P. Simon, J. Power Sources 196 (2011) 1620–1625.
[15] X. Dong, F. Lu, L. Yang, Y. Zhang, X. Wang, Mater. Chem. Phys. 112 (2) (2008) 596–602.
[16] X. Xu, Z. Wen, X. Yang, L. Chen, Mater. Res. Bull. 43 (8–9) (2008) 2334–2341.
[17] E.D. Botto, C. Bourbon, S. Patoux, P. Rozier, M. Dolle, J. Power Sources 196 (2011) 2274–2278.
[18] A. Aboulaich, R. Bouchet, G. Delaizir, V. Seznec, L. Tortet, M. Morcrette, P. Rozier, J.M. Tarascon, V. Viallet, M. Dollé, Adv. Eng. Mater. 1 (2) (2011) 179–183.
[19] K. Takada, Acta Mater. 61 (3) (2013) 759–770.
[20] J.-M. Tarascon, M. Armand, Nature 414 (2001) 359–367.
[21] B. Scrosati, J. Garche, J. Power Sources 195 (9) (2010) 2419–2430.
[22] J.B. Goodenough, Y. Kim, Chem. Mater. 22 (3) (2010) 587–603.
[23] A. Mukhopadhyay, A. Tokranov, F. Guo, X. Xiao, R.H. Hurt, B.W. Sheldon, Adv. Funct. Mater. 23 (19) (2013) 2397–2404.
[24] A. Mukhopadhyay, A. Tokranov, X. Xiao, B.W. Sheldon, Electrochim. Acta 66 (2012) 28–37.
[25] A. Mukhopadhyay, A. Tokranov, K. Sena, X. Xiao, B.W. Sheldon, Carbon 49 (8) (2011) 2742–2749.
[26] A.K. Shukla, T.P. Kumar, Curr. Sci. 94 (3) (2008) 314–331.
[27] W.J. Zhang, J. Power Sources 196 (1) (2011) 13–24.
[28] A.S. Arico, P. Bruce, B. Scrosati, J.-M. Tarascon, W.V. Schalkwijk, Nat. Mater. 4 (2005) 366–377.
[29] V.S. Saji, Y.-S. Kim, T.-H. Kim, J. Cho, H.-K. Song, Phys. Chem. Chem. Phys. 13 (43) (2011) 19226–19237.
[30] H.K. Liu, G.X. Wang, Z.P. Guo, J.Z. Wang, K. Konstantinov, J. New Mater. Electrochem. Syst. 10 (2007) 101–104.
[31] R. Mukherjee, R. Krishnan, Toh-Ming Lu, N. Koratkar, Nano Energy 1 (4) (2012) 518–533.
[32] Y. Kobayashi, H. Miyashiro, T. Takeuchi, H. Shigemura, N. Balakrishnan, M. Tabuchi, H. Kageyama, T. Iwahori, Solid State Ionics 152–153 (2002) 137–142.
[33] V. Etacheri, R. Marom, R. Elazari, G. Salitra, D. Aurbach, Energy Environ. Sci. 4 (2011) 3243–3262.
[34] H. Takahara, T. Takeuchi, M. Tabuchi, H. Kageyama, Y. Kobayashi, Y. Kurisu, S. Kondo, R. Kanno, J. Electrochem. Soc. 151 (10) (2004) A1539–A1544.
[35] G. Delaizir, V. Viallet, A. Aboulaich, R. Bouchet, L. Tortet, V. Seznec, M. Morcrette, J.-M. Tarascon, P. Rozier, M. Dollé, Adv. Funct. Mater. 22 (2012) 2140–2147.
[36] N. Kamaya, K. Homma, Y. Yamakawa, M. Hirayama, R. Kanno, M. Yonemura, T. Kamiyama, Y. Kato, S. Hama, K. Kawamoto, A. Mitsui, Nat. Mater. 10 (2011) 682–686.
[37] S. Ahmad, Ionics 15 (2009) 309–321.
[38] J.W. Fergus, J. Power Sources 195 (15) (2010) 4554–4569.
[39] J.Y. Song, Y.Y. Wang, C.C. Wan, J. Power Sources 77 (2) (1999) 183–197.
[40] A.M. Stephan, K.S. Nahm, Polymer 47 (16) (2006) 5952–5964.
[41] J.-M. Tarascon, A.S. Gozdz, C. Schmutz, F. Shokoohi, P.C. Warren, Solid State Ionics 86–88 (1) (1996) 49–54.
[42] A. Ghosh, C. Wang, P. Kofinas, J. Electrochem. Soc. 157 (7) (2010) A846–A849.
[43] V. Thangadurai, W. Weppner, Ionics 12 (2009) 81–92.
[44] P. Knauth, Solid State Ionics 180 (14–16) (2009) 911–916.
[45] S.C. Li, Z.X. Lin, Solid State Ionics 9–10 (2) (1983) 835–838.
[46] H. Aono, E. Sugimoto, Y. Sadaoka, N. Imanaka, G. Adachi, J. Electrochem. Soc. 137 (4) (1990) 1023–1027.
[47] H. Aono, E. Sugimoto, Y. Sadaoka, N. Imanaka, G. Adachi, Solid State Ionics 40-41 (1) (1990) 38–42.
[48] H. Aono, E. Sugimoto, Y. Sadaoka, N. Imanaka, G. Adachi, Solid State Ionics 47 (3–4) (1991) 257–264.
[49] K. Ado, Y. Saito, T. Asai, H. Kageyama, O. Nakamura, Solid State Ionics 53–56 (2) (1992) 723–727.
[50] Y. Kobayashi, T. Takeuchi, M. Tabuchi, K. Ado, H. Kageyama, J. Power Sources 81–82 (1999) 853–858.
[51] C.M. Chang, Y. Il Lee, S.H. Hong, J. Am. Ceram. Soc. 88 (7) (2005) 1803–1807.
[52] X.X. Xu, Z.Y. Xu, J.G. Wu, X.L. Yang, Solid State Ionics 178 (1–2) (2007) 29–34.
[53] M.A. Subramanian, R. Subramanian, A. Clearfield, Solid State Ionics 18–19 (1) (1986) 562–569.
[54] S. Duluard, A. Paillassa, L. Puech, P. Vinatier, V. Turq, P. Rozier, P. Lenormand, P.-L. Taberna, P. Simon, F. Ansart, J. Eur. Ceram. Soc. 33 (6) (2013) 1145–1153.
[55] Z. Wen, X. Xu, J. Li, J. Electroceram. 22 (2009) 342–345.
[56] J. Schoonman, Solid State Ionics 135 (1–4) (2000) 5–19.
[57] C.M. Chang, S.H. Hong, H.-M. Park, Solid State Ionics 176 (35–36) (2005) 2583–2587.
[58] A. Mei, Q.H. Jiang, Y.H. Lin, C.W. Nan, J. Alloys Compd. 486 (1–2) (2009) 871–875.
[59] C.H. Chen, K. Amine, Solid State Ionics 144 (2001) 51–57.
[60] Y.-X. Gao, X.-P. Wang, Q.-X. Sun, Z. Zhuang, Q.-F. Fang, Front. Mater. Sci. 6 (3) (2012) 216–224.
[61] Y.-X. Gao, X.-P. Wang, W.G. Wang, Z. Zhuang, D.M. Zhang, Q.-F. Fang, Solid State Ionics 181 (2010) 1415–1419.
[62] R. Murugan, W. Weppner, P. Schmid-Beurmann, T. Venkataraman, Mater. Sci. Eng. B 143 (2007) 14–20.
[63] Z. Liu, F. Huang, Z. Cao, J. Yang, M. Liu, Y. Wang, Mater. Lett. 62 (8–9) (2008) 1366–1368.
[64] J. Maier, Prog. Solid State Chem. 23 (3) (1995) 171–263.
[65] A.K. Padhi, K.S. Nanjundaswamy, J.B. Goodenough, J. Electrochem. Soc. 144 (4) (1997) 1188–1194.
[66] A. Yamada, S.C. Chung, K. Hinokuma, J. Electrochem. Soc. 148 (3) (2001) A224–A229.
[67] S. Okada, S. Sawa, M. Egashira, J. Yamaki, M. Tabuchi, H. Kageyama, T. Konishi, A. Yoshino, J. Power Sources 97–98 (2001) 430–432.
[68] P.P. Prosini, M. Carewska, S. Scaccia, P. Wisniewski, S. Passerini, M. Pasquali, J. Electrochem. Soc. 149 (7) (2002) A886–A890.
[69] H. Huang, S.-C. Yin, L.F. Nazar, Electrochem. Solid-State Lett. 4 (10) (2001) A170–A172.
[70] S. Okada, M. Ueno, Y. Uebou, J.-I. Yamaki, J. Power Sources 146 (1–2) (2005) 565–569.
[71] Y. Arachi, Y. Higuchi, R. Nakamura, Y. Takagi, M. Tabuchi, J. Power Sources 244 (2013) 631–635.
[72] K.J. Takeuchia, A.C. Marschilok, S.M. Davis, R.A. Leising, E.S. Takeuchi, Coordin. Chem. Rev. 219–221 (2001) 283–310.
[73] J. Wang, X. Sun, Energy Environ. Sci. 5 (1) (2012) 5163–5185.
[74] T. Takeuchi, M. Tabuchi, K. Ado, K. Tatsumi, J. Power Sources 174 (2007) 1063–1068.
[75] T. Takeuchi, M. Tabuchi, A. Nakashima, H. Kageyama, K. Tatsumi, Electrochem. Solid-State Lett. 8 (4) (2005) A195–A198.
[76] T. Takeuchi, M. Tabuchi, A. Nakashima, T. Nakamura, Y. Miwa, H. Kageyama, K. Tatsumi, J. Power Sources 146 (1–2) (2005) 575–579.
[77] T. Takeuchi, H. Sakaebe, H. Kageyama, H. Senoh, T. Sakai, K. Tatsumi, J. Power Sources 195 (9) (2010) 2928–2934.
[78] T. Takeuchi, H. Kageyama, K. Nakanishi, M. Tabuchi, H. Sakaebe, T. Ohta, H. Senoh, T. Sakai, K. Tatsumi, J. Electrochem. Soc. 157 (11) (2010) A1196–A1201.
[79] M.N. Obrovac, J.R. Dahn, Electrochem. Solid-State Lett. 5 (4) (2002) A70–A73.
[80] K. Biswas, A. Mukhopadhyay, B. Basu, K. Chattopadhyay, J. Mater. Res. 22 (6) (2007) 1491–1501.
[81] J.-S. Lee, C.-M. Chang, Y.I. Lee, J.-H. Lee, S.-H. Hong, J. Am. Ceram. Soc. 87 (2) (2004) 305–307.
[82] N. Gupta, A. Mukhopadhyay, K. Pavani, B. Basu, Mater. Sci. Eng. A 534 (2012) 111–118.
[83] K.M. Reddy, A. Mukhopadhyay, B. Basu, J. Eur. Ceram. Soc. 30 (2010) 3363–3375.
[84] Y. Mo, S.P. Ong, G. Ceder, Chem. Mater. 24 (2012) 15–17.
[85] S. Kondo, K. Takada, Y. Yamamura, Solid State Ionics 53 (1992) 1183–1186.